Journal of Geoscience and Environment Protection, 2022, 10, 327-339
https://www.scirp.org/journal/gep
ISSN Online: 2327-4344
ISSN Print: 2327-4336

Delineation of Near Surface Water Flow Path of Wahawa Geothermal Field by Using 2D Inversion of Resistivity Data

S. A. Samaranayake[1,2*], Nalin De Silva[3], U. Dahanayake[4], H. O. Wijewardane[4], N. D. Subasinghe[2]

[1]National Ocean Affairs Committee, Ministry of Foreign Relations, Colombo, Sri Lanka
[2]National Institue of Fundamental Studies, Kandy, Sri Lanka
[3]Geological Survey and Mines Bureau, Pitakotte, Sri Lanka
[4]Faculty of Applied Sciences, Rajarata University of Sri Lanka, Anuradhapura, Mihintale
Email: *samaranayakerusl@gmail.com

How to cite this paper: Samaranayake, S. A., De Silva, N., Dahanayake, U., Wijewardane, H. O., & Subasinghe, N. D. (2022). Delineation of Near Surface Water Flow Path of Wahawa Geothermal Field by Using 2D Inversion of Resistivity Data. *Journal of Geoscience and Environment Protection, 10,* 327-339.
https://doi.org/10.4236/gep.2022.108020

Received: September 12, 2021
Accepted: August 28, 2022
Published: August 31, 2022

Abstract

The Wahawa geothermal field which is located in the Eastern province of Sri Lanka has an average temperature of 60˚C in its surface manifestations. Since the temperature is considerably high, it is important to explore the feasibility of direct utilization of the energy of this geothermal field. In the present study, electrical resistivity measurements were employed in a 20 km^2 region in order to delineate the Wahawa geothermal system and to understand the near-surface fracture pattern. Electrical resistivity mapping of the region has been carried out using Schlumberger array measurements with nominal current array spacing (half spacing) of 150 m and it was observed that there was a path of low (<30 W) apparent resistivity. These results revealed that the hotsprings resting on a hard rock terrain are presumably composed of metamorphic rocks, suggesting lateral movement of hotwater towards the hotsprings instead of a deep-influx. The area of surface manifestations is not suitable for utilization application due to clustering of the main feeding path. The major hotwater feeding path which is extending in the west direction can be recommended as a possible drilling target for direct utilization applications.

Keywords

Electrical Resistivity, Fracture, Direct Utilization, Surface Manifestation

1. Introduction

Heat from the deep earth is exposed to the surface in many ways; the conductive

heat flow through the crust, volcanic eruptions, and as heated water. Hotsprings are the features resulting when ground water is heated by geothermal forces and brought to the surface (Hochstein, 1988). The occurrences of hotsprings are not rare in many geological settings in the world, since the Earth is tectonically active with plate margins and active faults. Water in the subsurface is heated basically by two methods. One method is that the water percolating deep into the earth may be heated up under normal geothermal conditions and pumped up to the surface, retaining the heat of the water. The other method is that the near-surface magmatic body or a volcano may act as a source to heat up water at shallow depths giving rise to hotsprings. Also, a slight change of water temperature may occur due to biogenic processes, with no correlation to the heat at depths (Bjorn, 2016). According to the setting of the heat source, there are two types of heat flow patterns that can be identified in a geothermal field (**Figure 1**). They are the heat source immediately beneath the surface manifestation and vertical heat flow path to the surface (Cox et al., 2015; Barnes & Rose, 1998) and the heat flow in the direction of long-running angle fractures (Kresic, 2010; Kumara & Dharmagunawardhane, 2014).

Detailed information about water flow pattern of the hotspring is crucial for harnessing heat for direct utilization. In particular, this is especially important for demarcating near surface drilling targets. Therefore, this study was focused on understanding the near surface water flow path of the Wahawa geothermal field, which can be identified as one of the suitable geothermal fields for direct utilization applications in Sri Lanka.

The gravity, magnetic and electrical methods play a vital role in geothermal exploration (Shah et al., 2015; Kiyak et al., 2015; Kana et al., 2015). Gravity and magnetic surveys are used to identify the geological structures and related geological features in the field (Blakely, 1996; Hinze et al., 2013). Resistivity techniques

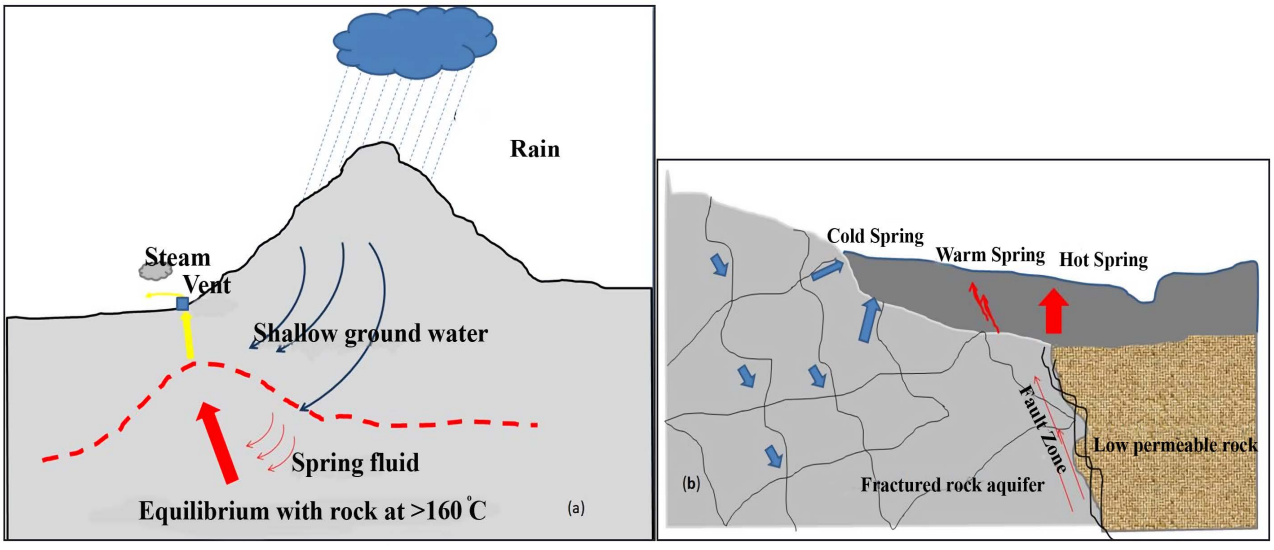

Figure 1. Types of hotsprings according to the feeding paths. (a) Heat source just beneath the surface manifestation and vertical heat flow path to the surface (After Cox et al., 2015); (b) heat flow toward the long running angle fractures (After Kresic, 2010).

are used to identify subsurface fracture patterns and reservoir characteristics (Palacky, 1988; Samaranayake et al., 2015). Among the resistivity methods, Direct Current (DC) resistivity method is employed for low depths (Zohdy et al., 1973). Therefore, the majority of geothermal exploration relies on magnetotellurics (Li et al., 2015; Nimalsiri et al., 2015). The broad objective of this study was to delineate the near surface fracture pattern and hence a DC resistivity method was employed (Roy & Apparao, 1971).

2. Geological Setting

Sri Lanka is an island in the Indian Ocean, near the equator, between 5˚55'N to 9˚55'N latitudes and 79˚42'E to 81˚52'E longitudes. The geographical location of Sri Lanka is comparatively far from known active tectonic plate boundaries. Nearly 90% of Sri Lanka is underlain by late Proterozoic high-grade metamorphic rocks (Kehelpannala, 1997). Three major litho tectonic units are defined based on Nd model ages namely the Highland complex (HC), the Wanni complex (WC), and the Vijayan complex (VC) within the high grade metamorphic basement (Nimalsiri et al., 2015) (**Figure 2**).

The actual contact between HC and VC is difficult to locate precisely due to lack of outcrops, but there is evidence for a tectonic thrust between them. Geothermal surface manifestations have been recorded in several places in Sri Lanka, where it can be seen that a NS trending belt of hot springs lines up with the lithological boundary of the HC in the west and the VC in the east.

Wahawa thermal springs are located approximately 1 km away from the HC-VC boundary on the VC side. The area is generally flat with few outcrops. The lithology of units underlying the terrain is composed of hornblende biotite and the study area is characterized by a number of fractures and faults (**Figure 3**). The prominent fracture trends in the NE-SW direction and it makes up the lineament governing the structure of the area. A major dolerite dyke is passing through the study site in a NW-SE direction. The shear zone is driven perpendicular to the dyke. The geothermal field is located in close proximity to the area, where dolerite dykes and the shear zone intersect. Apart from that, there are no prominent geological features visible in the area of interest. Wahawa geothermal field consists of more than 10 surface manifestations. The surface temperature of each hotspring is different from one another, with an average 60˚C surface temperature.

3. Methodology

Electrical resistivity measurements are used in an investigation of a 20 km^2 region in order to delineate the Wahawa geothermal system and to understand the near-surface fracture pattern. Electrical resistivity mapping of the region has been carried out using Schlumberger array measurements with nominal current array (half) spacing of 150 m. **Figure 4** shows the electrode setup of the Schlumberger array. Resistivity measured by the Schlumberger array can be

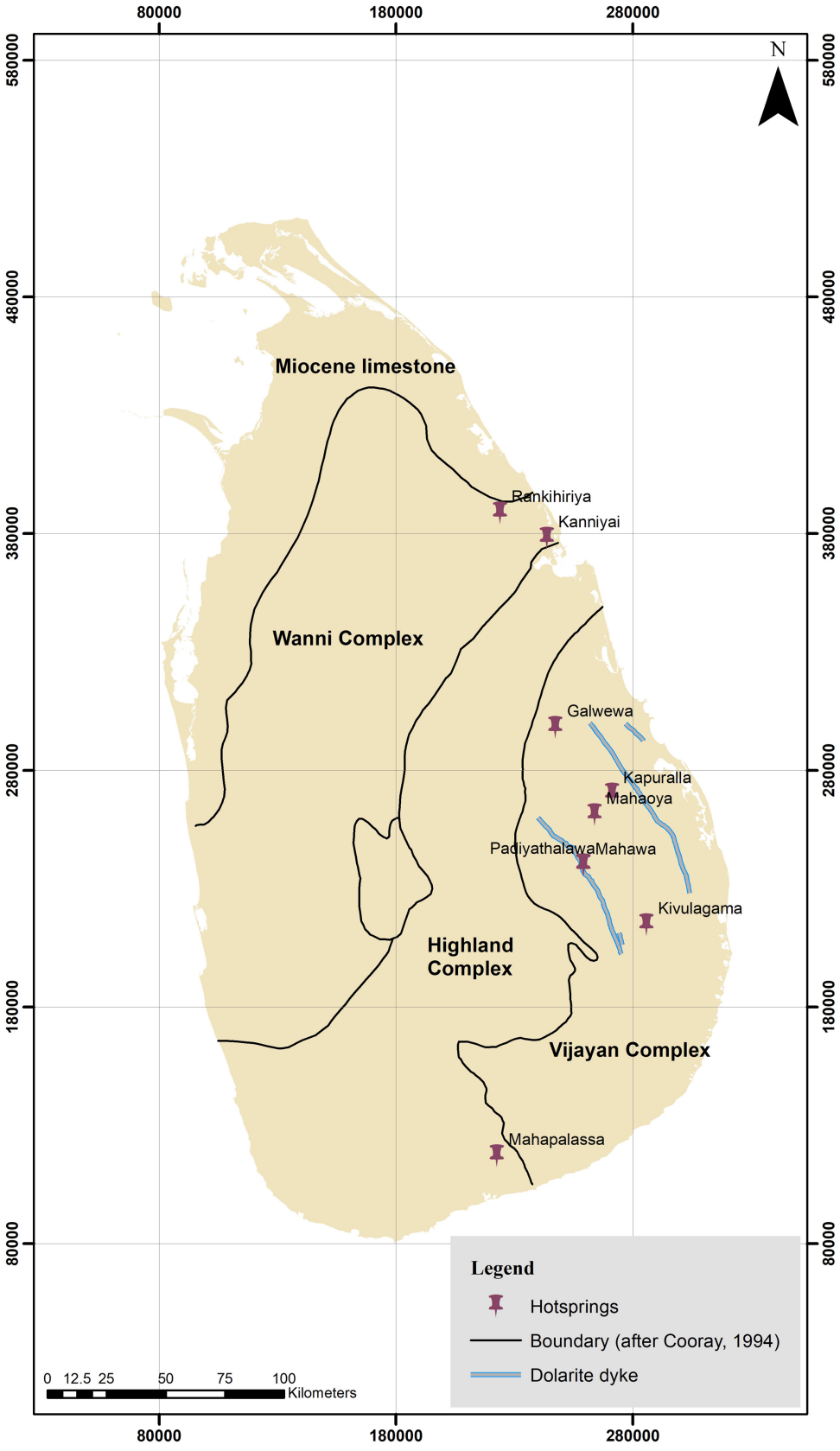

Figure 2. Geological setting of Sri Lanka. Major crustal subdivisions, locations of the hot spring systems.

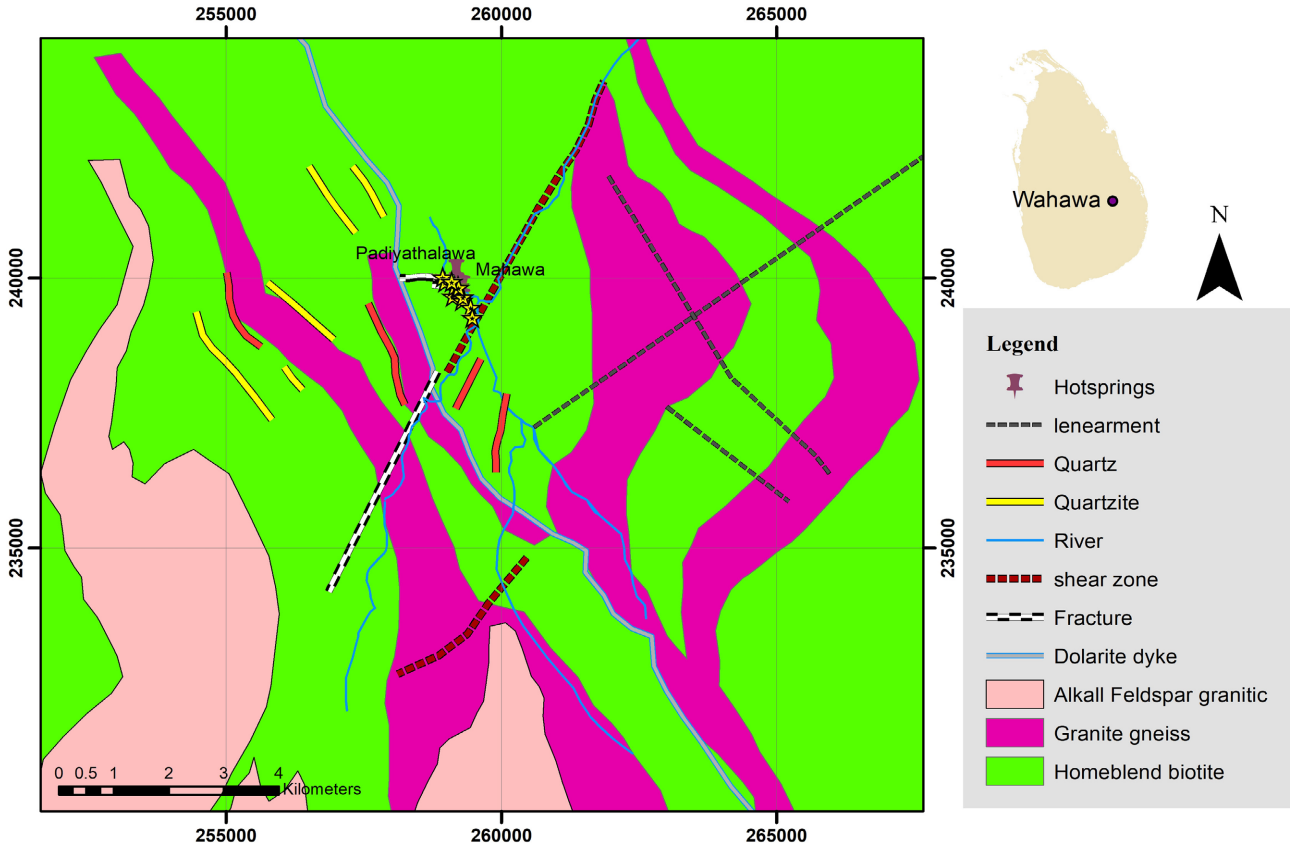

Figure 3. Geological features around Wahawa thermal spring system, (After Geological Survey and Mines Bureau of Sri Lanka, 2011).

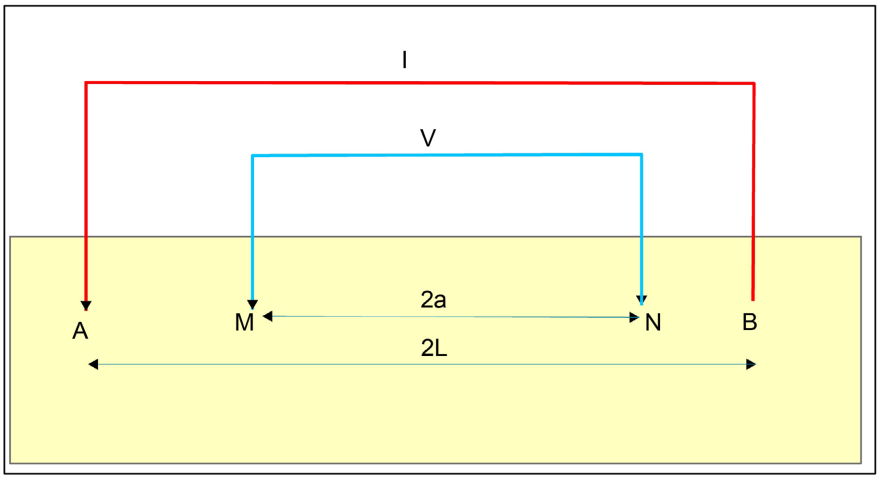

Figure 4. Electrode setup of the Schlumberger array.

expressed as

$$\rho = \pi \frac{\Delta V}{2I\left(L^2 - a^2\right)}, \tag{1}$$

where

ρ = resistivity

ΔV = Potential difference

I = Current.

According to Equation (1) and Figure 4, "a" is half of the potential electrode distance [MN/2] and L is half of the current electrode distance [AB/2] (Telford et al., 1990; Reynolds, 2011; Everett, 2013). Advanced Geosciences, Inc. (AGI) mini string 2D resistivity imaging system with 28 electrodes is used for 2D data acquisition.

The hotsprings of the geothermal field are roughly aligned with the NW-SE direction and appear in the shear zone which is driven in the same direction. Therefore, the EW direction was selected for main profiling and the NS direction was selected for cross profiling. These cross lines were used to control the quality of the profiling. 26 2D profiles were obtained and resistivity profile setup is shown in Figure 5. 1D resistivity profiles were conducted to enhance the data quality by cross checking with 2D profiles.

4. Results

Twenty six (26) 2D profiles were obtained and they were categorized into 5 zones (A, B, C, D, and E) according to the geology of the area (Figure 5).

Zone A: This is the Western end of the survey area and the dolerite dyke is also located in this zone. Five 2D profiles (each 270 m long) were conducted in this zone and the resistivity profiles are shown in Figure 6. According to the resistivity images of 2D profiles, there are no indications for fractures in the Zone

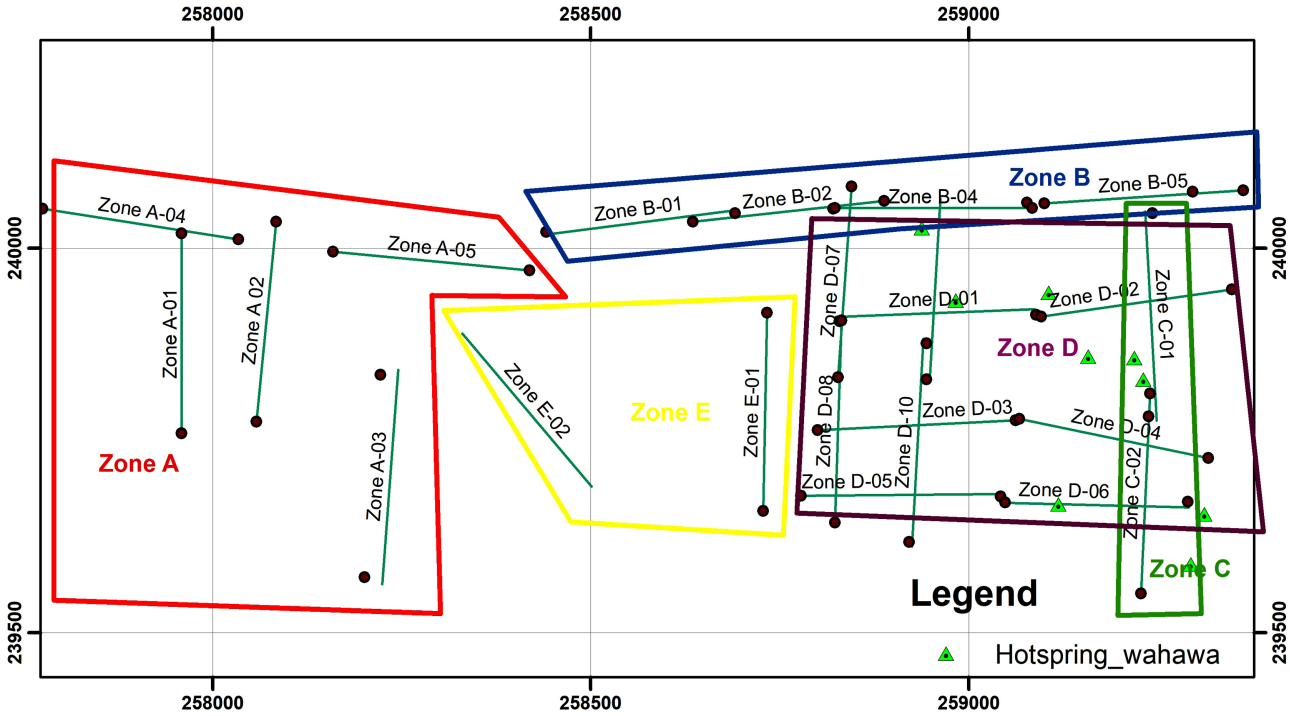

Figure 5. 2D resistivity profiles and vertical electrical sounding locations of Wahawa geothermal field; The survey chategarized in to 5 zones and display as Zone A (blue polygon), Zone B (green polygon), Zone C (pink polygon), Zone D (purple polygon) and Zone E (yellow polygon).

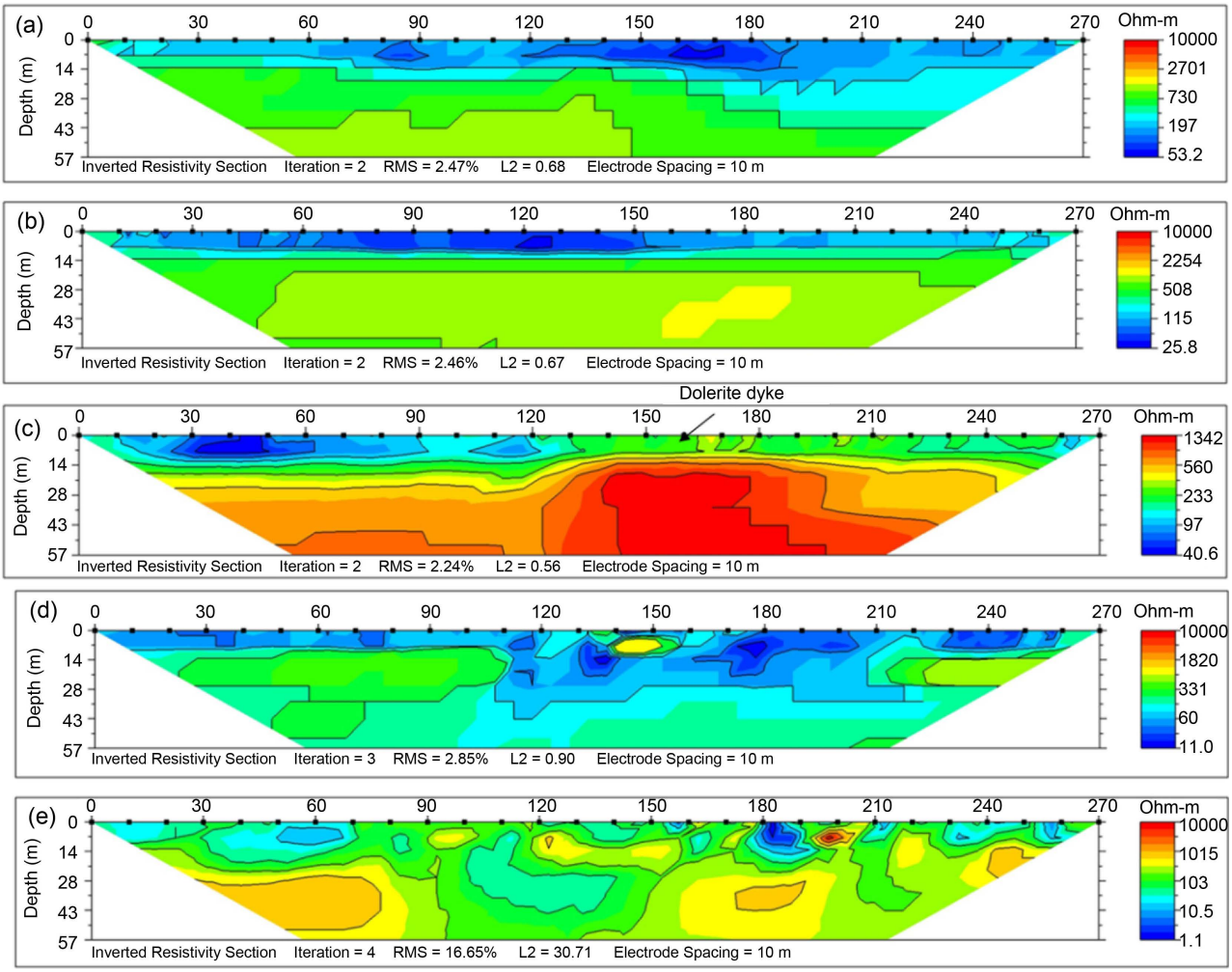

Figure 6. 2D resistivity profile in Zone A; (a): Zone A-01, (b): Zone A-02, (c): Zone A-03, (d): Zone A-04, (e): Zone A-05.

A in the western side of the dolerite dyke.

Zone B: Northern end of the survey area is categorized as Zone B and 5 2D resistivity profiles were conducted in this area. These profiles were set up in line, so that they overlap with each other to obtain better results. The profile setting and 2D profiles are shown in Figure 7. Zone B-01 and Zone B-02 images very clearly show the presence of (comparatively) low resistivity zones. Since they occur alternatively, they clearly indicate fracture zones (probably joints) in the rock weathered at shallow depth. They must be tight as they extend to depths and therefore, do not appear as low resistive zones towards depths. This is because high resistivity of country rocks dominates towards depth. The results clearly show that the northern end is acting as a barrier for near-surface fracture propagation.

Zone C: Zone C covers the eastern side of the geothermal field. According to the terrain condition, only 2 profiles were conducted along the direction NS. Figure 8 shows the line setup and 2D profiles of Zone C. There are some fractures notable in the 2D profiles indicating the continuation of fracture in South

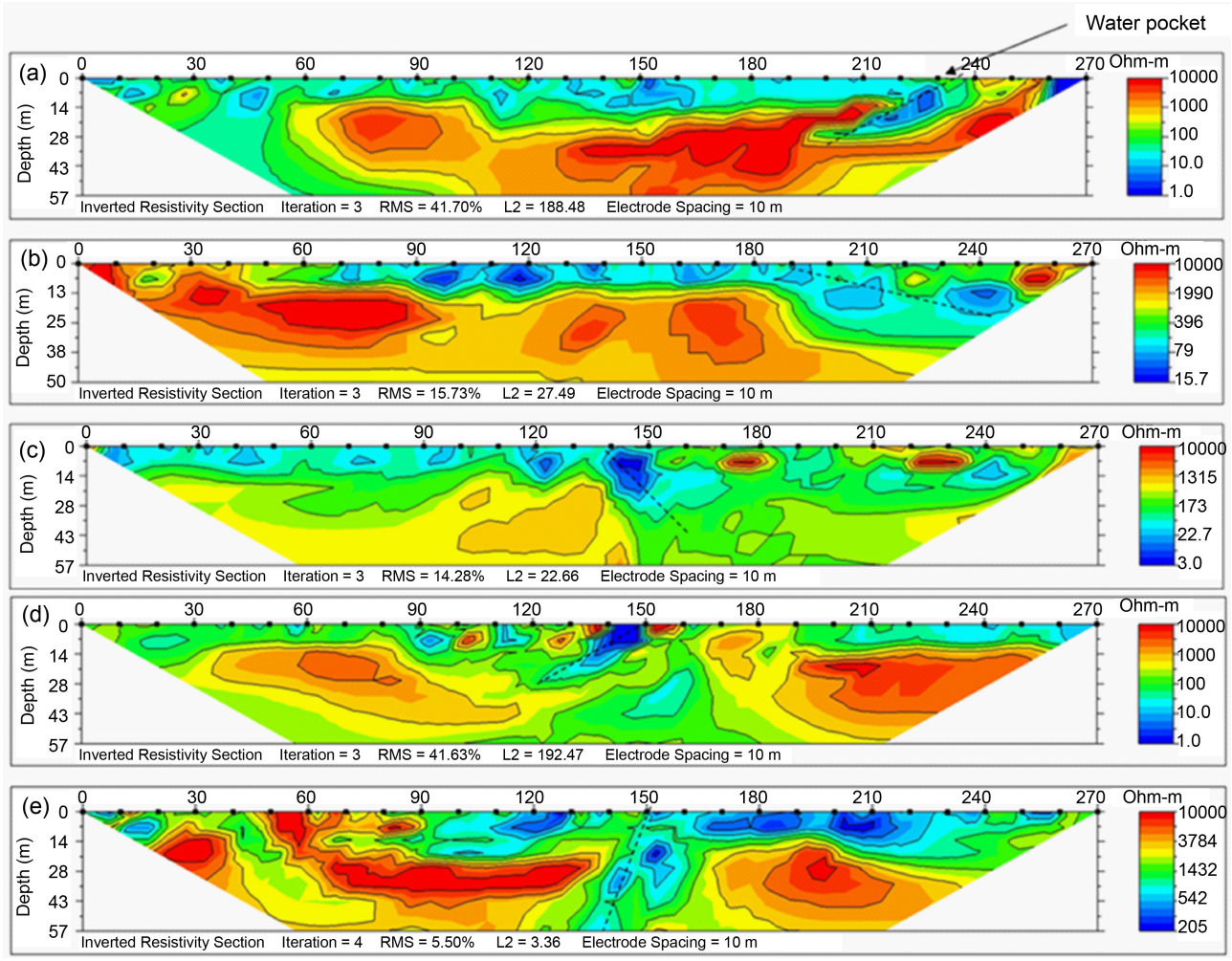

Figure 7. 2D resistivity profiles in Zone B; (a): Zone B-01, (b): Zone B-02, (c): Zone B-03, (d): Zone B-04, (e): Zone B-05.

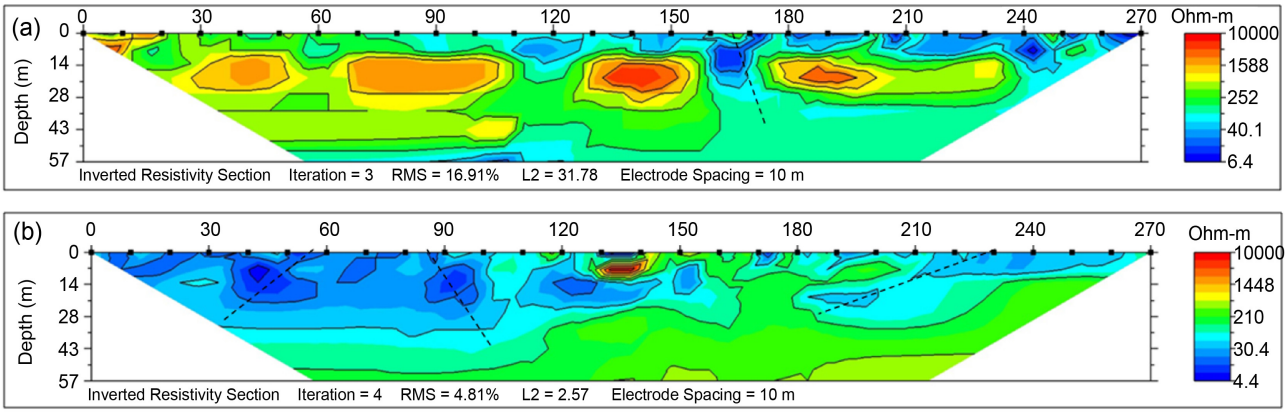

Figure 8. Resistivity profile in Zone C: (a): Zone C-01, (b): Zone C-02.

East direction. 2D resistivity results (Figure 8), show a number of small fractures through the area indicating the clustering of main fracture. The sharp wide fracture noted in the western side of zone gives some evidence for main fracture that is fed to the geothermal manifestations. Therefore, an extension

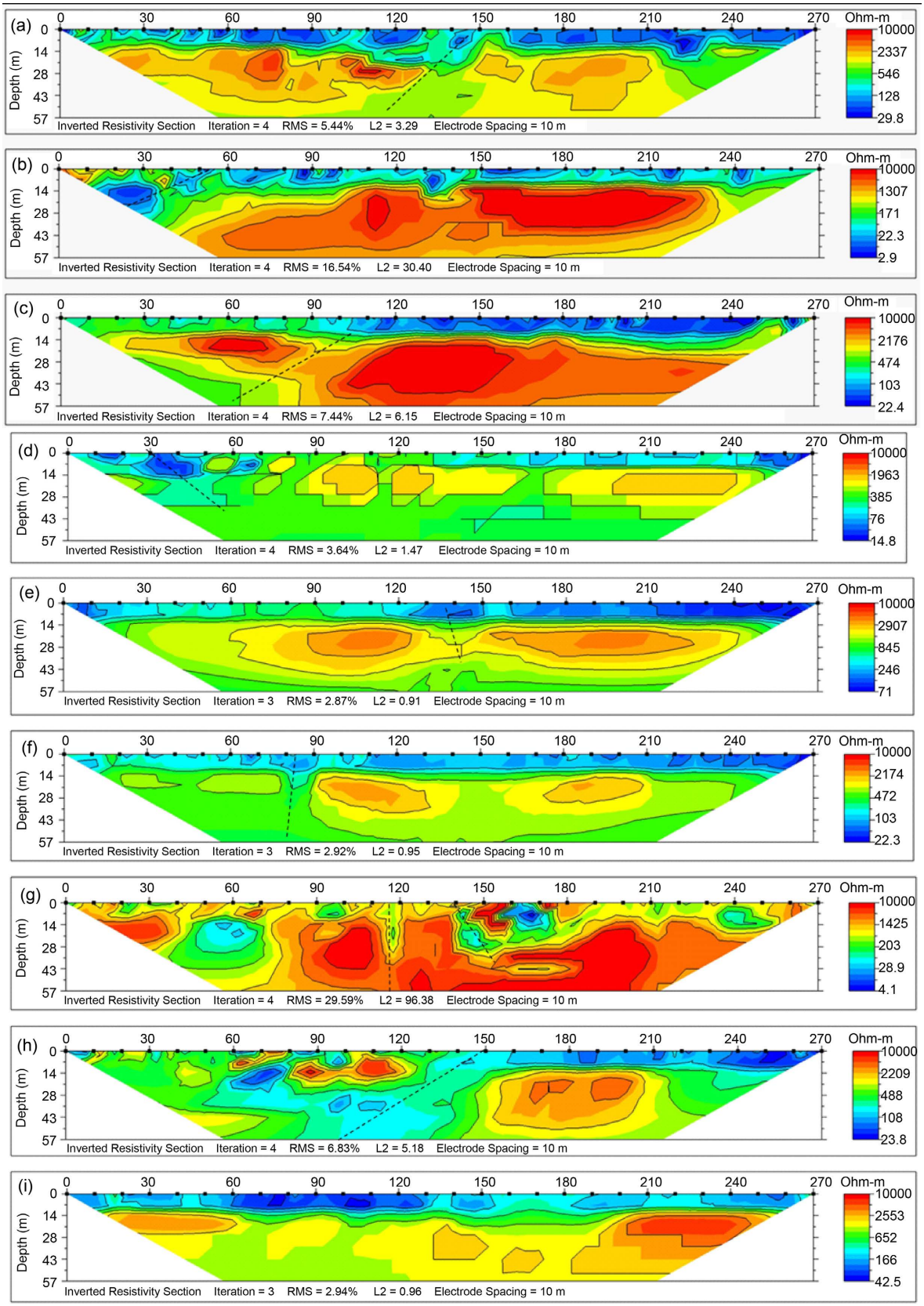

Figure 9. 2D resistivity profiles in Zone D; (a): Zone D-01, (b): Zone D-02, (c): Zone D-03. (d): Zone D-04, (e): Zone D-05, (f): Zone D-06, (g): Zone D-07, (h): Zone D-08, (i): Zone D-09.

of west boundary (Zone D) was considered to detect fracture propagation.

Zone D: ZoneD is in the area of the hotsprings. This area was surveyed as a grid to understand the near surface characteristics of the hotspring field. The layout of the profiles is shown in Figure 9. There are some near surface fractures noted in figures of Zone D-04, Zone D-06, Zone D-07 and Zone D-08 indicating the clustering of main fracture.

Zone E: Extension of western margin of Zone D is named as Zone E. Two (02)2D profiles were conducted accordingly to understand the fracture propagation. The 2D resistivity structures of the Zone E profiles are shown in Figure 10. Results show that the major fracture continued up to the dolerite dyke and disappears, probably due to deepening of the fracture after the dolerite dyke.

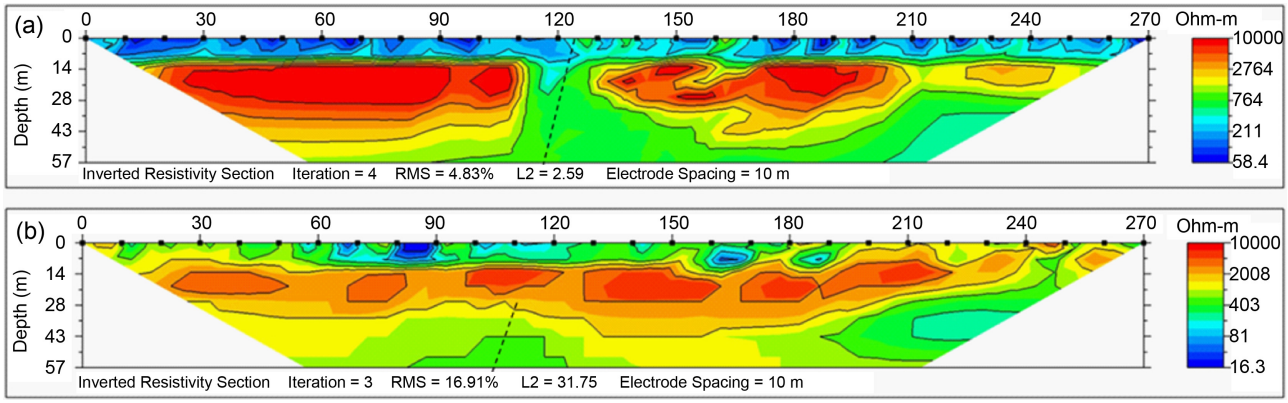

Figure 10. 2D resistivity profiles in Zone E; (a): Zone E-01, (b): Zone E-02, (c): Zone E-03.

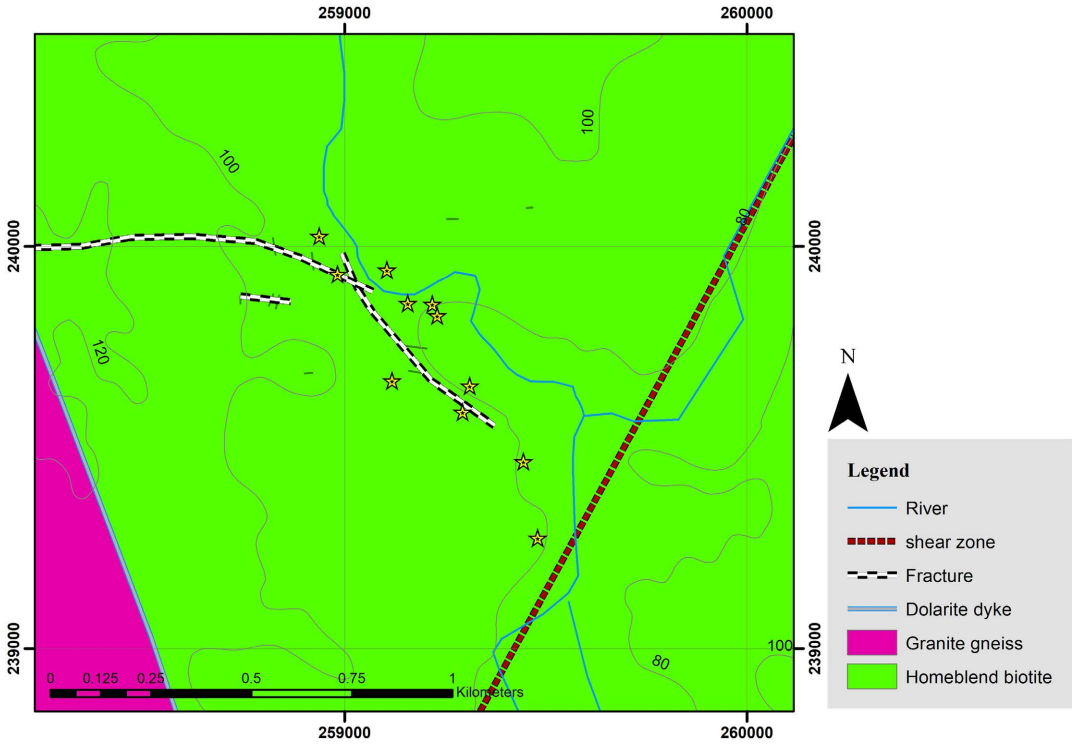

Figure 11. Fracture continuation demarcated in 2D resistivity survey.

5. Discussion

The interpretation of the 2D resistivity profiles shows that the Wahawa geothermal springs area has geo-electric layers with low, moderate, and relatively high resistivity zones that could result in from high resistive rocks and fractures.

The resistivity imaging survey has also mapped different weak zones through which the geothermal fluids discharge to the surface. The resistivity data shows the presence of deep extending fracture zone in the hotspring area. The fracture extends to the North West direction starting from the spring field as shown in Figure 11. Then it is further bends to the south direction and passes through the spring field. These fracture zones can act as pathways to thermal water from depths. In addition, the Wahawa geothermal spring is associated with a major fracture which is found to be oriented in the west direction, where both the dolerite dyke and the H/V boundary are located.

6. Conclusion

In this study, it was intended to understand the near-surface water flow path of the Wahawageothermal springs in Sri Lanka using a resistivity method. The near subsurface of the locality of thermal springs marked by a low resistive zone indicates the channeling of major fracture in the area of surface manifestations. The NW extension from this low resistive area shows the feeding fracture continuation. The impermeable metamorphic basement located in other cardinal directions with higher resistivity indicates the absence of feeding fracture zones in those directions. The current analysis revealed that the feeding fracture of the Wahawa geothermal field is a western trending dipping fracture and extending up to the dolerite dyke. The results of this study could be used for the direct utilization applications, particularly to identify the drilling targets.

Acknowledgements

Authors acknowledge the support given for this study by Professor C.B. Dissanayake, Mr. T.B. Nimalsiri, and Mr. N.B. Suriyaarchchi National Institue of Fundamental Studies, Hantana Road, Kandy, Sri Lanka.

Conflicts of Interest

The authors declare no conflicts of interest regarding the publication of this paper.

References

Barnes, H. L., & Rose, A. W. (1998). Origins of Hydrothermal Ores. *Science, 279,* 2064-2065. https://doi.org/10.1126/science.279.5359.2064

Bjorn, S. (2016). *Medium Enthalpy Geothermal Systems in Iceland—Thermal and Electric Potential.* Ísor-2016/008, Iceland Geosurvey / National Energy Authority of Iceland-technical Report.

Blakely, R. J. (1996). *Potential Theory in Gravity and Magnetic Applications.* Cambridge

University Press. https://doi.org/10.1017/CBO9780511549816

Cox, S. C., Menzies, C. D., Sutherland, R., Denys, P. H., Chamberlain, C., & Teagle, D. A. (2015). Changes in Hot Spring Temperature and Hydrogeology of the Alpine Fault Hanging Wall, New Zealand, Induced by Distal South Island Earthquakes. *Geofluids, 15,* 216-239. https://doi.org/10.1111/gfl.12093

Everett, M. E. (2013). *Near-Surface Applied Geophysics*. Cambridge University Press. https://doi.org/10.1017/CBO9781139088435

Geological Survey and Mines Bureau of Sri Lanka (2011). *Geology Map of Padiyatalawa—Tampaddi, Sheet 15, 1:100000, Provisional Map Series*.

Hinze, W. J., Von Frese, R. R., Von Frese, R., & Saad, A. H. (2013). *Gravity and Magnetic Exploration: Principles, Practices, and Applications*. Cambridge University Press. https://doi.org/10.1017/CBO9780511843129

Hochstein, M. P. (1988). Assessment and Modelling of Geothermal Reservoirs (Small Utilization Schemes). *Geothermics, 17,* 15-49. https://doi.org/10.1016/0375-6505(88)90004-1

Kana, J. D., Djongyang, N., Raïdandi, D., Nouck, P. N., & Dadjé, A. (2015). A Review of Geophysical Methods for Geothermal Exploration. *Renewable and Sustainable Energy Reviews, 44,* 87-95. https://doi.org/10.1016/j.rser.2014.12.026

Kehelpannala, K. V. W. (1997). Deformation of a High-Grade Gondwana Fragment, Sri Lanka. *Gondwana Research, 1,* 47-68. https://doi.org/10.1016/S1342-937X(05)70005-8

Kıyak, A., Karavul, C., Gülen, L., Pekşen, E., & Kılıç, A. R. (2015). Assessment of Geothermal Energy Potential by Geophysical Methods: Nevşehir Region, Central Anatolia. *Journal of Volcanology and Geothermal Research, 295,* 55-64. https://doi.org/10.1016/j.jvolgeores.2015.03.002

Kresic, N. (2010). Chapter 2. Types and Classifications of Springs. In N. Kresic, & Z. Stevanovic (Eds.), *Groundwater Hydrology of Springs* (pp. 31-85). Butterworth-Heinemann. https://doi.org/10.1016/B978-1-85617-502-9.00002-5 https://www.sciencedirect.com/science/article/pii/B9781856175029000025

Kumara, S. M. P. G. S., & Dharmagunawardhane, H. A. (2014). A Geostructural Model for the Nelumwewa Thermal Spring: North Central Province, Sri Lanka. *Journal of Geological Society of Sri Lanka, 16,* 19-27.

Li, H., Xiao, P., Yu, J., & Lyu, H. (2015). Magnetotelluric Interpretation of the Geothermal Structure of Xiongjing Area, China. *SEG Technical Program Expanded Abstracts 2015* (pp. 2047-2050). Society of Exploration Geophysicists. https://doi.org/10.1190/segam2015-5906871.1

Nimalsiri, T. B., Suriyaarachchi, N. B., Hobbs, B., Manzella, A., Fonseka, M., Dharmagunawardena, H. A., & Subasinghe, N. D. (2015). Structure of a Low-Enthalpy Geothermal System Inferred from Magnetotellurics—A Case Study from Sri Lanka. *Journal of Applied Geophysics, 117,* 104-110. https://doi.org/10.1016/j.jappgeo.2015.03.025

Palacky, G. J. (1988). Resistivity Characteristics of Geologic Targets. In M. N. Nabighian (Ed.), *Electromagnetic Methods in Applied Geophysics* (Vol. 1, pp. 53-129). Society of Exploration Geophysicists. https://doi.org/10.1190/1.9781560802631.ch3

Reynolds, J. M. (2011). *An Introduction to Applied and Environmental Geophysics*. John Wiley & Sons.

Roy, A., & Apparao, A. (1971). Depth of Investigation in Direct Current Methods. *Geophysics, 36,* 943-959. https://doi.org/10.1190/1.1440226

Samaranayake, S. A., De Silva, S. N., Dahanayake, U., Wijewardana, H. O., & Subasinghe, N. D. (2015). Feasibility of Finding Geothermal Sources in Sri Lanka with Reference to

the Hot Spring Series and the Dolerite Dyke. *Proceedings of World Geothermal Congress 2015*. International Geothermal Association.

Shah, M., Sircar, A., Vaidya, D., Sahajpal, S., Chaudhary, A., & Dhale, S. (2015). Overview of Geothermal Surface Exploration Methods. *International Journal of Advance Research and Innovative, 1,* 55-64.

Telford, W. M., Geldart, L. P., Sheriff, R. E., & Sheriff, R. E. (1990). *Applied Geophysics*. Cambridge University Press. https://doi.org/10.1017/CBO9781139167932

Zohdy, A. A. R., Anderson, L. A., & Muffler, L. J. P. (1973). Resistivity, Self-Potential, and Induced-Polarization Surveys of a Vapor-Dominated Geothermal System. *Geophysics, 38,* 1130-1144. https://doi.org/10.1190/1.1440400